

Original Research

Early Detection of Risk of Neo-Sinus Blood Stasis Post-Transcatheter Aortic Valve Replacement Using Personalized Hemodynamic Analysis



Seyedvahid Khodaei, PhD^a , Mohamed Abdelkhalik, MASc^b , Nima Maftoon, PhD^{c,d},
Ali Emadi, PhD^{a,e} , Zahra Keshavarz-Motamed, PhD^{a,b,f,*}

^a Department of Mechanical Engineering, McMaster University, Hamilton, Ontario, Canada

^b School of Biomedical Engineering, McMaster University, Hamilton, Ontario, Canada

^c Department of Systems Design Engineering, University of Waterloo, Waterloo, Ontario, Canada

^d Centre for Bioengineering and Biotechnology, University of Waterloo, Waterloo, Ontario, Canada

^e Department of Electrical and Computer Engineering, McMaster University, Hamilton, Ontario, Canada

^f School of Computational Science and Engineering, McMaster University, Hamilton, Ontario, Canada

ARTICLE INFO

Article history:

Submitted 23 December 2022

Revised 27 February 2023

Accepted 1 March 2023

Available online 28 April 2023

Keywords:

Cardiac fluid dynamics

Coronary hemodynamics

Global hemodynamics

Patient-specific lumped parameter model

Transcatheter aortic valve replacement

Valve thrombosis local fluid dynamics

ABSTRACT

Background: Despite the demonstrated benefits of transcatheter aortic valve replacement (TAVR), subclinical leaflet thrombosis and hypoattenuated leaflet thickening are commonly seen as initial indications of decreased valve durability and augmented risk of transient ischemic attack.

Methods: We developed a multiscale patient-specific computational framework to quantify metrics of global circulatory function, metrics of global cardiac function, and local cardiac fluid dynamics of the aortic root and coronary arteries.

Results: Based on our findings, TAVR might be associated with a high risk of blood stagnation in the neo-sinus region due to the lack of sufficient blood flow washout during the diastole phase (e.g., maximum blood stasis volume increased by 13, 8, and 2.7 fold in the left coronary cusp, right coronary cusp, and noncoronary cusp, respectively [N = 26]). Moreover, in some patients, TAVR might not be associated with left ventricle load relief (e.g., left ventricle load reduced only by 1.2 % [N = 26]) and diastolic coronary flow improvement (e.g., maximum coronary flow reduced by 4.94%, 15.05%, and 23.59% in the left anterior descending, left circumflex coronary artery, and right coronary artery, respectively, [N = 26]).

Conclusions: The transvalvular pressure gradient amelioration after TAVR might not translate into adequate sinus blood washout, optimal coronary flow, and reduced cardiac stress. Noninvasive personalized computational modeling can facilitate the determination of the most effective revascularization strategy pre-TAVR and monitor leaflet thrombosis and coronary plaque progression post-TAVR.

ABBREVIATIONS

3D, 3-dimensional; AS, aortic stenosis; CT, computed tomography; DE, Doppler echocardiography; HALT, hypoattenuated leaflet thickening; LAD, left anterior descending; LCC, left coronary cusp; LCX, left circumflex; LV, left ventricle; NCC, noncoronary cusp; RCA, right coronary artery; RCC, right coronary cusp; TAVR, transcatheter aortic valve replacement.

Introduction

As transcatheter aortic valve replacement (TAVR) has moved to the forefront of valvular interventions, certain complications have emerged. Most recently, clinical or subclinical valve thrombosis (detected by hypoattenuated leaflet thickening or HALT) has been shown to restrict

valve leaflet mobility and increase the risk of early valve deterioration or consequent embolic stroke.^{1–3} The prevalence of leaflet thrombosis and subclinical HALT is uncertain, with reported frequencies up to 30% for leaflet thrombosis⁴ and up to 40% for HALT⁵ in the literature. Despite those unfavorable trends, there is still no clear understanding of the hemodynamic details and correlations with clinical outcomes.^{6–8}

* Address correspondence to: Zahra Keshavarz-Motamed, PhD, McMaster University, Department of Mechanical Engineering (Mail to JHE-310), Hamilton, Ontario, Canada L8S 4L7.

E-mail address: motamedz@mcmaster.ca (Z. Keshavarz-Motamed).

Our understanding of the occurrence of leaflet thrombosis and HALT in TAVR patients is restricted, and the link between leaflet thrombosis and hemodynamics is obscure.⁹ After TAVR, an immediate decrease in transvalvular pressure gradient is likely as a result of aortic stenosis (AS) removal. However, the correlation between HALT and aortic valve hemodynamics is uncertain, with some studies suggesting a correlation between HALT and reduced leaflet motion/elevated pressure gradient^{10,11} and others suggesting otherwise.^{6,8} Therefore, the diagnosis of a positive HALT is primarily based on the observed reduced leaflet motion through computed tomography (CT) imaging. However, most patients are asymptomatic and repeated CT scans can be harmful for a vast majority of the patients.^{6,12} While anticoagulation is currently the standard treatment for HALT, there is ongoing debate and uncertainty about the best antiplatelet and anticoagulation therapy.⁶ Therefore, there is a huge motivation to investigate hemodynamic features, such as flow stasis patterns, to predict blood stagnation on a case-by-case basis in order to assess the clinical consequences and the underlying fluid dynamic mechanisms of leaflet thrombosis risk.¹³

Long-term hemodynamic complications (such as leaflet thrombosis) can be diagnosed in early stages using computational modeling.^{14,15,16} Accurate diagnosis relies on quantifying certain requirements: **global** hemodynamics (1) cardiac function metrics (e.g., heart workload) and breakdowns of each cardiovascular disease element's hemodynamics and **local** hemodynamics (2) aortic root and coronary arteries fluid dynamics (e.g., 3-dimensional [3D] flow information). In this study, we developed a diagnostic computational framework (using a patient-specific image-based lumped parameter algorithm and computational fluid dynamics) to investigate the impact of TAVR on both local and global hemodynamics to investigate the progression of thrombotic process after TAVR (Figure 1). We used the clinically measured hemodynamic metrics of 26 patients in both pre- and post-TAVR conditions to provide novel hemodynamic analysis and interpretations of clinical data (Figures 2–7). To the best of our knowledge, this is the first study that investigated the effects of TAVR on blood thrombosis in terms of both local and global hemodynamics.

Methods

Study Population

Among a cohort of 250 patients, 26 patients with severe AS who received TAVR (Table 1: patient characteristics) and underwent a follow-up echo and CT post-TAVR were retrospectively selected from anonymized databases between 2020 and 2022 at the Hamilton General Hospital in Hamilton, Ontario, Canada. Patients' selections for post-TAVR CT were done by the heart team blinded to the study objectives, excluding those with either medical (e.g., substantial possibility of contrast nephropathy) or social (e.g., unable to go or refused to take part) impediments to executing the follow-up CT. In addition, those treated for surgical aortic bioprostheses degeneration (i.e., valve-in-valve) and those with unsuccessful devices as per VARC-2 (Valve Academic Research Consortium) criteria were excluded.¹⁷ Other exclusion criteria were any patient data with missing required inputs for the computational modeling. We did not exclude any data based on image quality. All discrepancies were sorted out by communicating with the local investigators. The protocols were reviewed and approved by the Hamilton Integrated Research Ethics Board and informed consents were collected from all participants. Measurements were obtained according to guidelines including American Heart Association, American College of Cardiology, and American Society of Echocardiography.^{18,19} Data were collected at both preprocedure and postprocedure time points. Results were expressed as mean \pm standard deviations.

Doppler Echocardiography

Doppler echocardiography (DE) data included the measurements and reports that were collected preprocedure and at postprocedure.

Echocardiograms and reports were reviewed and analyzed in a blinded fashion by senior cardiologists using OsiriX imaging software (OsiriX version 8.0.2; Pixmeo, Bernex, Switzerland).

Computed Tomography

CT images of the patients (both pre- and post-TAVR) were used to segment and reconstruct the 3D geometries. Detailed information regarding geometry reconstruction is outlined in the [Supplemental Materials](#).

Statistical Analysis

For the variables presented in this study, baseline patient information is reported as number (percentages) for categorical variables and mean \pm standard deviation or median (interquartile range) for continuous variables depending on normality. Continuous variables were tested for normality using the Shapiro-Wilk test. Correlations between the continuous variables were performed using parametric Pearson's r or nonparametric Spearman's ρ . Paired samples t -tests were performed on pre-post TAVR variables using Mann-Whitney U or Wilcoxon W depending on normality. Statistical significance based on the corresponding test's p -value was considered as follows (medium $p < 0.05$; strong $p < 0.01$; very strong $p < 0.001$). All analyses were performed using Jamovi (v.1.8).

Numerical Study

Global Hemodynamics

We have previously developed a Doppler-based patient-specific lumped parameter algorithm to quantify global hemodynamics for complex valvular, vascular, mini-vascular, and ventricular disease (3V-lumped parameter model)^{20,21} (Figure 1, Supplemental Table 1) in both pre- and post-TAVR conditions (See Supplemental Materials). The model uses a limited number of input parameters, all of which can be reliably obtained using DE (e.g., stroke volume, heart rate, ejection time, ascending aorta area, aortic valve effective orifice area, and aortic regurgitation effective orifice area) and a sphygmomanometer (systolic and diastolic blood pressures). Note that the proposed method does not need catheter data for calculation of left ventricle (LV) workload or the other hemodynamics parameters. The computed LV workload in our study is the integral of LV pressure and its volume change (calculated by our lumped parameter algorithm) and was estimated as the area covered by the LV pressure–volume (P-V) loop. The developed framework was validated against cardiac catheterization data with a considerable inter- and intra-patient variability with a broad range of diseases in a population of forty-nine patients (with AS).²⁰ Moreover, some of the sub-models of the patient-specific lumped parameter algorithm have been used previously,^{20,22–31} with validation against in vivo cardiac catheterization^{32,33} in patients with vascular diseases, in vivo magnetic resonance imaging data³⁴ in patients with AS, and in vivo magnetic resonance imaging data^{35–37} in patients with mixed valvular diseases and coarctation.

Local Hemodynamics

We developed a fluid-solid interaction and lumped parameter modeling framework to calculate 3D blood flow dynamics in all main coronary artery branches (left main coronary artery, left anterior descending [LAD], left circumflex [LCX], and right coronary artery [RCA]), aortic root, ascending aorta, sinus, and neo-sinus regions for both pre- and post-TAVR (Figure 1) (See Supplemental Materials). Our patient-specific lumped parameter model and 3D fluid-solid interaction modeling (used to compute local hemodynamics) were validated against in vivo DE data as explained in Khodaei et al.^{22,24,38} and Keshavarz-Motamed et al.³⁹

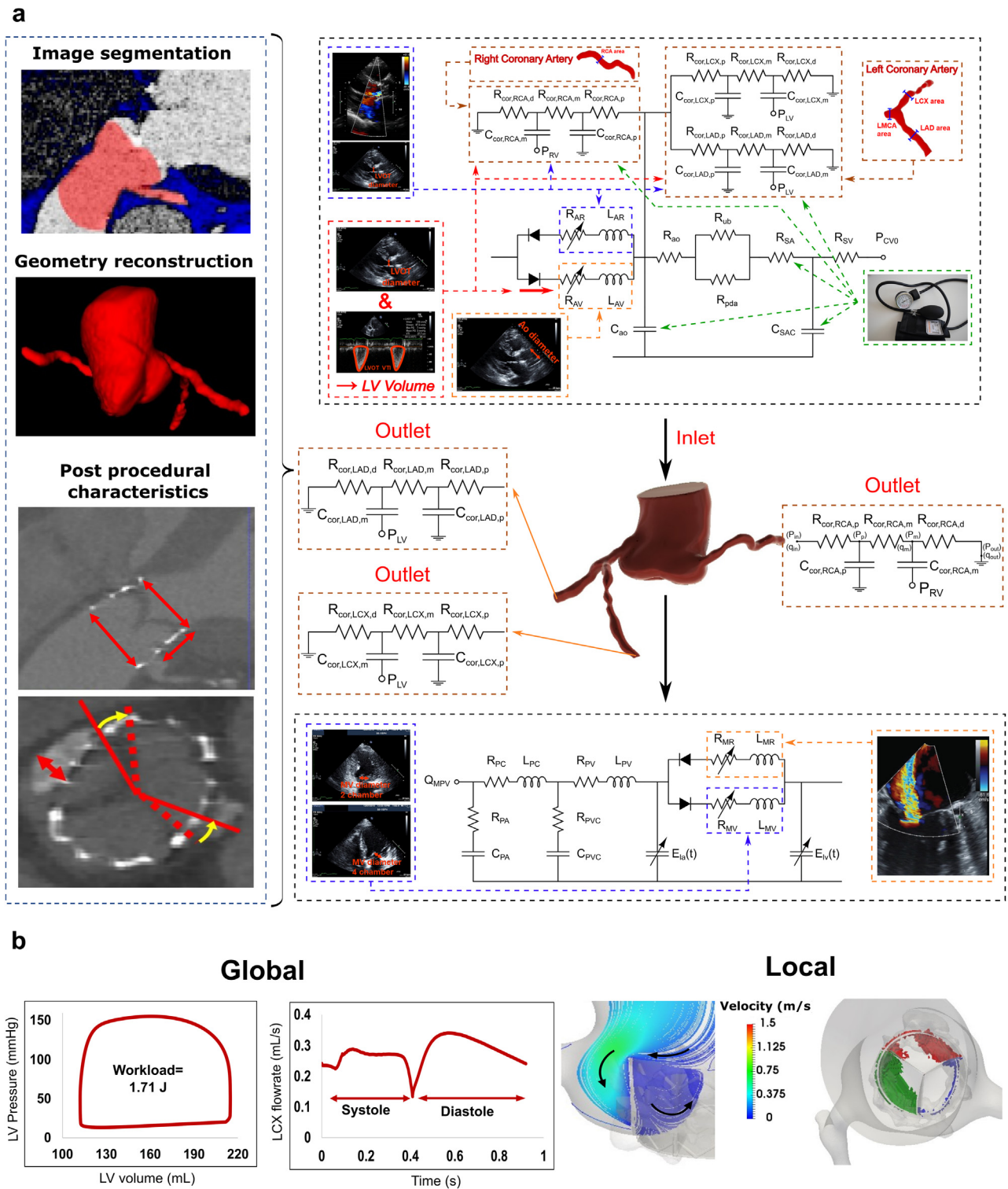


Figure 1. (a) Schematic of computational domain. This model incorporates the following sub-models. (1) ascending aorta and aortic root, (2) left ventricle, (3) left anterior descending coronary artery, (4) left circumflex coronary artery, and (5) right coronary artery. Abbreviations are the same as in Supplemental Table 1; (b) Sample results of local and global hemodynamic outputs produced by non-invasive computational framework.

Results

Blood Flow Stasis (Local)

The total amount of areas within the sinus and neo-sinus regions with velocity less than 0.001 m/s was determined for all patients as an indicator of halted blood flow which is associated with a great

risk of creating a thrombus layer on the leaflets.^{38,40,41} Our results demonstrated that for all individuals, regardless of their clinical state, TAVR procedure was linked to a significantly greater possibility of blood clotting and thrombus accumulation owing to the hampered washout of the aortic root and the irregular vortical structures (Figure 2). At the peak diastole, the stagnant volume of flow for the left coronary cusp (LCC) neo-sinus had an average

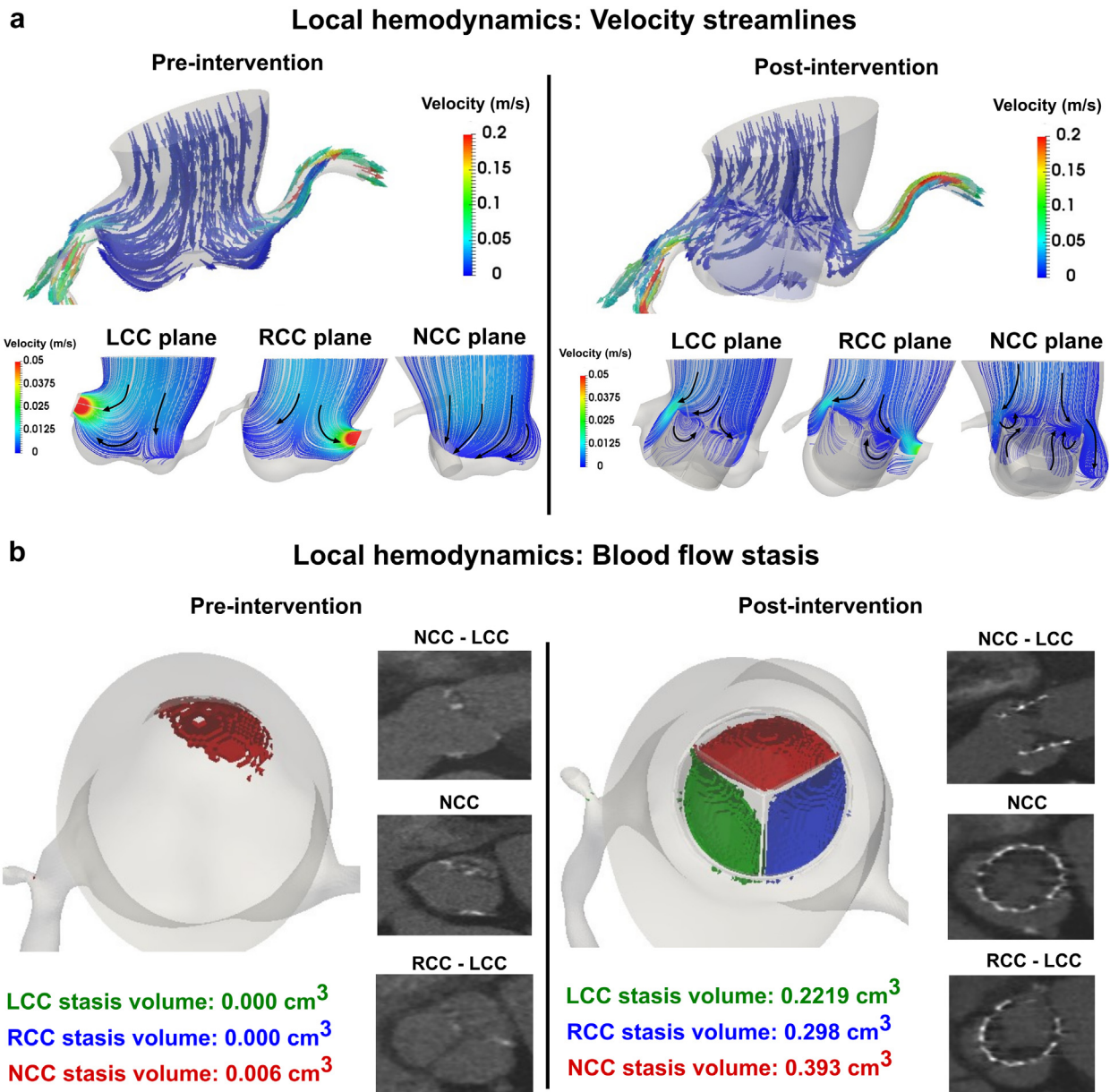


Figure 2. Local hemodynamics at baseline and post-TAVR in patient #21. (a) Blood flow vortical structure in the sinus and neo-sinus in the central plane of each leaflet during diastole in pre- and post-TAVR states; (b) Blood stasis volume per leaflet neo-sinus at peak diastole and CT-based evidence of hypoattenuated leaflet thickening on the leaflets. In patient #21, the disturbed vortical structure due to the malpositioning of prosthetic valve and its interaction with the coronary ostium inflow as well as anatomical alterations of aortic root impede the proper flow washout with significant increase of blood stasis volume post-TAVR.

Abbreviations: CT, computed tomography; LCC, left coronary cusp; NCC, noncoronary cusp; RCC, right coronary cusp; TAVR, transcatheter aortic valve replacement.

increase of over 13-fold ($t = 5.05$; $p < 0.001$), 8-fold for the right coronary cusp (RCC) neo-sinus ($t = 4.78$; $p < 0.001$), and 2.7-fold for noncoronary cusp (NCC) neo-sinus ($t = 4.78$; $p < 0.001$), resulting in a total increase of 4 times across all cups ($t = 5.86$; $p < 0.001$) (Figure 4a-d). Prior to and after TAVR, NCC faced an augmented risk of thrombosis (81% pre-TAVR and 56.5% post-TAVR). Following NCC, RCC experienced a heightened risk of thrombosis (13.5% pre-TAVR and 27.7% post-TAVR), with LCC being the least vulnerable to thrombosis (5.5% pre-TAVR and 15.8% post-TAVR). Interestingly, we noticed a similar pattern in the calcium volume division (calcium volume score) of leaflets, with NCC having the greatest calcium volume (44.8%), trailed by RCC (33%) and finally LCC with the least calcium amount out of all the cusps (22.2%) (Figure 4e).

Coronary Blood Flow (Global)

Even though it is anticipated that the inflow of blood to the coronary arteries would augment after the prosthetic valve implantation and AS obstruction removal, our results showed that diastolic flow decreased in many cases and only a slight increase in systolic flow occurred for each of the coronary branches (See Figure 3 for one patient sample). As shown in Figure 5, on average, the peak systole flow increased 6.4% and 21.38% for LAD and RCA, respectively, while it remained almost unchanged (<1%) for LCX. Also, the peak diastole flow decreased by 4.94%, 15.05%, and 23.59% for LAD, LCX, and RCA, respectively. When examining each case individually (Figure 5), it was observed that there were diverse trends among the patients with regard to the enhancement of coronary flow after TAVR.

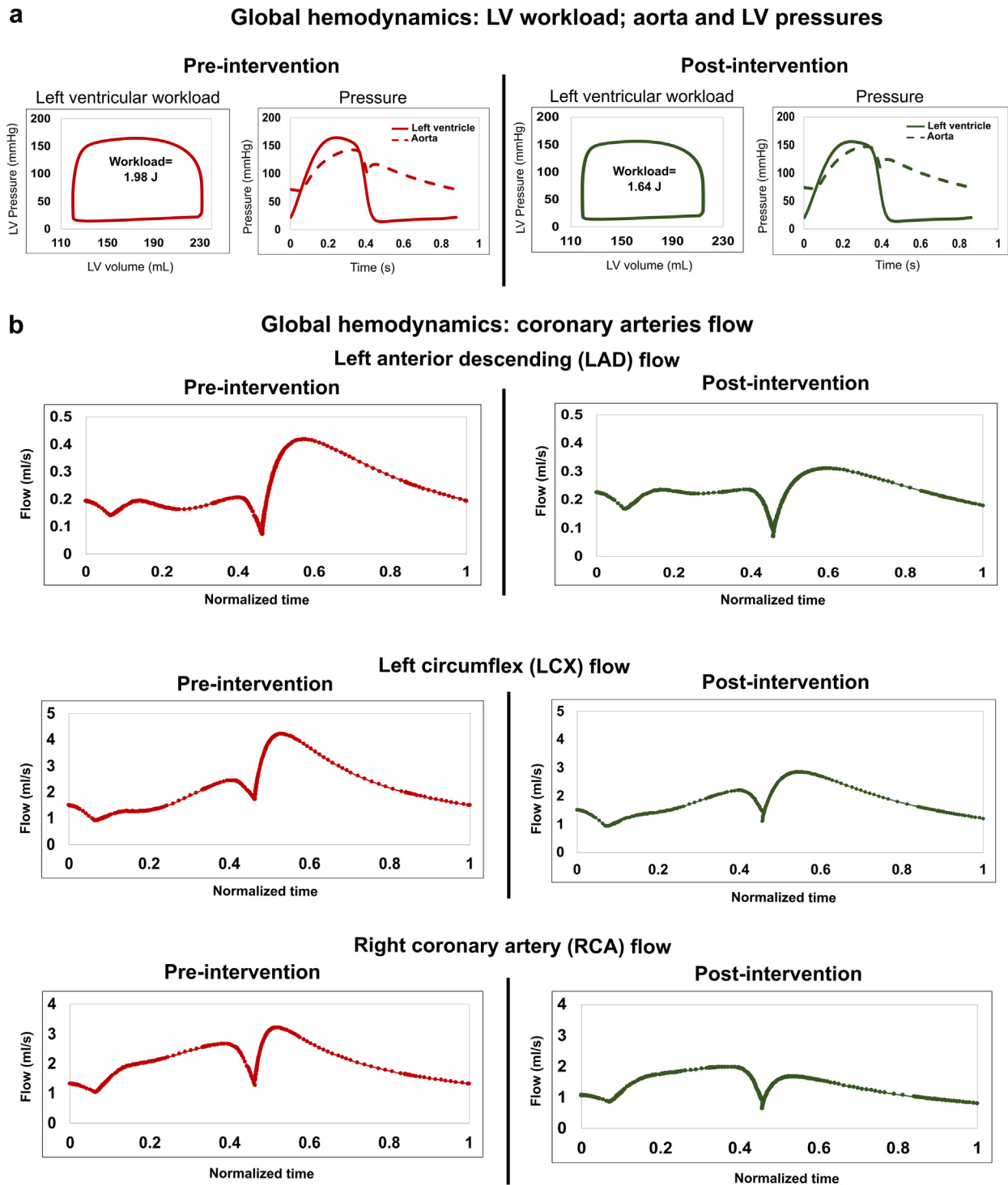


Figure 3. Global hemodynamics at baseline and post-TAVR in patient #21. (a) LV workload, LV and ascending aorta pressures; (b) Changes in computed coronary flowrate for LAD, LCX, and RCA branches pre- and post-TAVR. Abbreviations: LV, left ventricle; TAVR, transcatheter aortic valve replacement.

Left Ventricle Hemodynamics (Global)

The LV workload specifies the overall energy demanded by the ventricle to eject blood, which is a precise measure of LV load and clinical state.²⁰ The magnitude of the LV load is reliant on both the LV's pressure and its volume, and an overloaded LV (greater than 1J) is connected to disproportionate contribution of pressure and volume to LV's work.^{20,24} As an illustration, for patient #21 (Figure 3), the surplus

LV load after TAVR (1.64 J) was caused by persistent high pressure in LV (e.g., LV peak pressure was 155 mmHg post-TAVR). Despite the remarkable decrease in aortic valve pressure gradient as well as modest decrease in peak LV pressure for all patients following TAVR (Figure 6a and c), the LV workload failed to improve in more than half of the cases (Figure 6b). As shown in Figure 6, while on average, the aortic valve mean pressure gradient and peak LV pressure dropped by 63.14% ($t = 11.51$; $p < 0.001$) and 15.35% ($t = 6.04$; $p < 0.001$), respectively, after

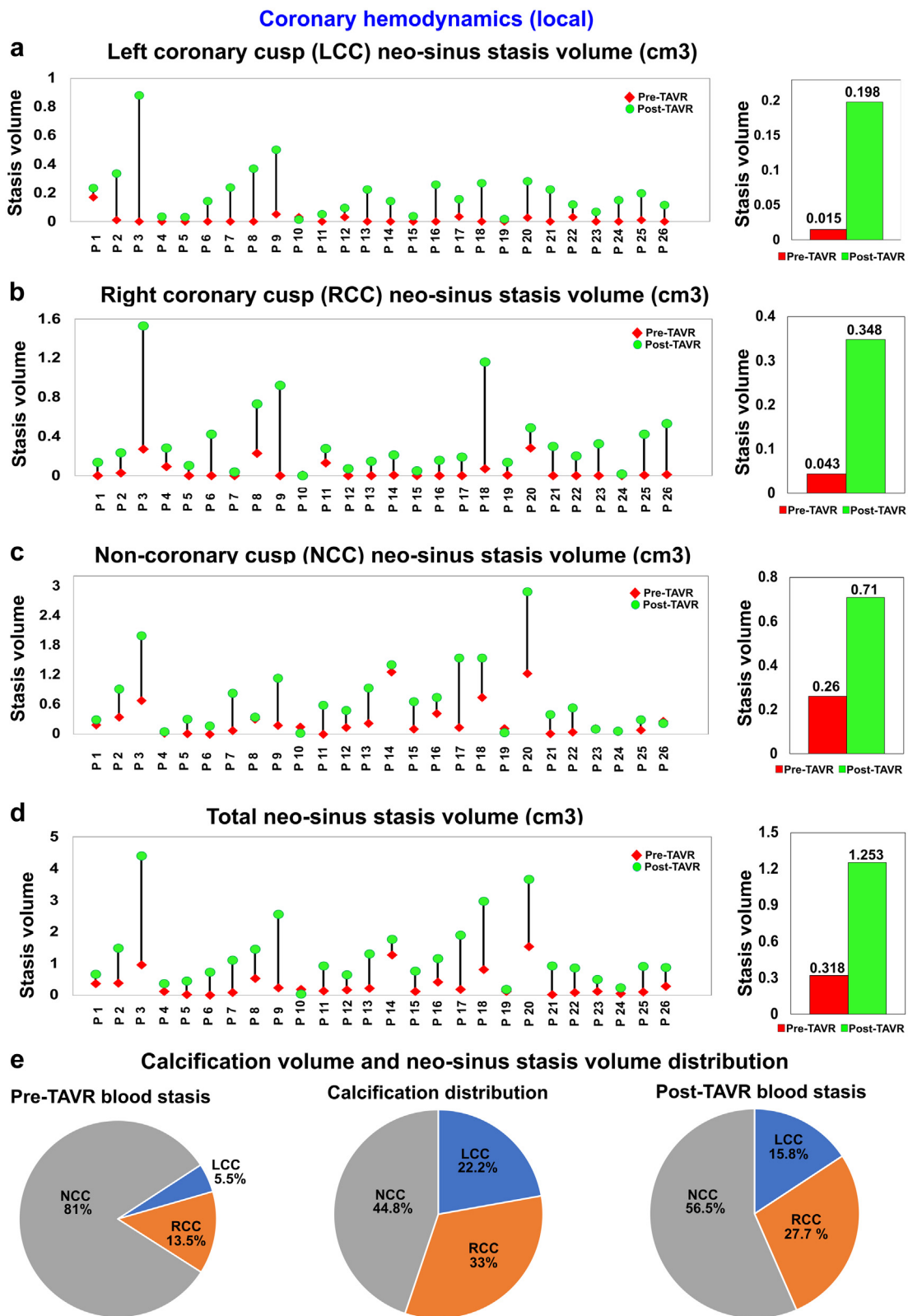


Figure 4. Local hemodynamics at baseline and post-TAVR (N = 26). (a) LCC neo-sinus stasis volume; (b) RCC neo-sinus stasis volume; (c) NCC neo-sinus stasis volume; (d) Total neo-sinus stasis volume; (e) Distributions of calcium volume per leaflet and blood stasis volume per leaflet pre- and post-TAVR. Abbreviations: LCC, left coronary cusp; NCC, noncoronary cusp; RCC, right coronary cusp; TAVR, transcatheter aortic valve replacement.

TAVR, the workload burden was not removed (only 1.2% decrease in workload [$t = 0.09$; $p = 0.929$]) after TAVR. Furthermore, it was observed that the workload of 20 patients (76.92% of the cases investigated in this study) was persistently greater than 1J post-TAVR,

signifying that the ventricle was overloaded after intervention. Among 26 patients in this study, the LV workload increased post-TAVR for 13 patients. In these 13 patients, post-TAVR, aortic regurgitation was worsened in 30%, mitral valve regurgitation was worsened

Coronary circulatory hemodynamics (global)

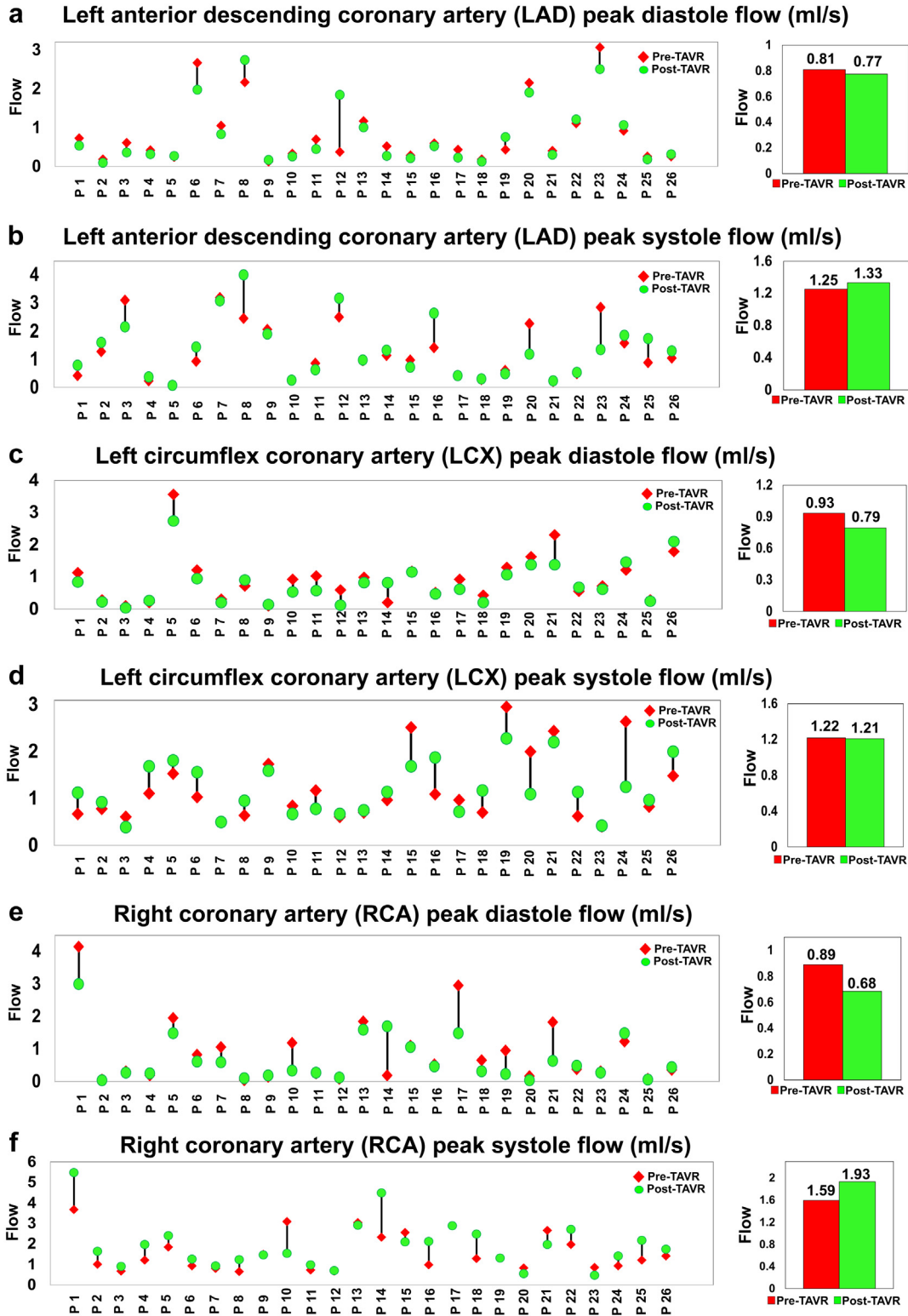


Figure 5. Local hemodynamics at baseline and post-TAVR (N = 26). (a) LAD peak diastolic flow; (b) LAD peak systolic flow; (c) LCX peak diastolic flow; (d) LCX peak systolic flow; (e) RCA peak diastolic flow; (f) RCA peak systolic flow. Abbreviation: TAVR, transcatheter aortic valve replacement.

in 30% of the cases, forward LV stroke volume increased in 77% of the cases, hypertension increased in 77% of the cases, the aortic valve effective orifice area did not change for 30% of the cases, and systemic compliance decreased in 54% of the cases.

Leaflets' Calcium Volumes vs. Hemodynamic Parameters (Local and Global)

We examined the correlation between the pre-TAVR calcium volume of the leaflets (LCC, RCC, and NCC) and hemodynamic parameters (local

Cardiac hemodynamics (global) and clinical metrics

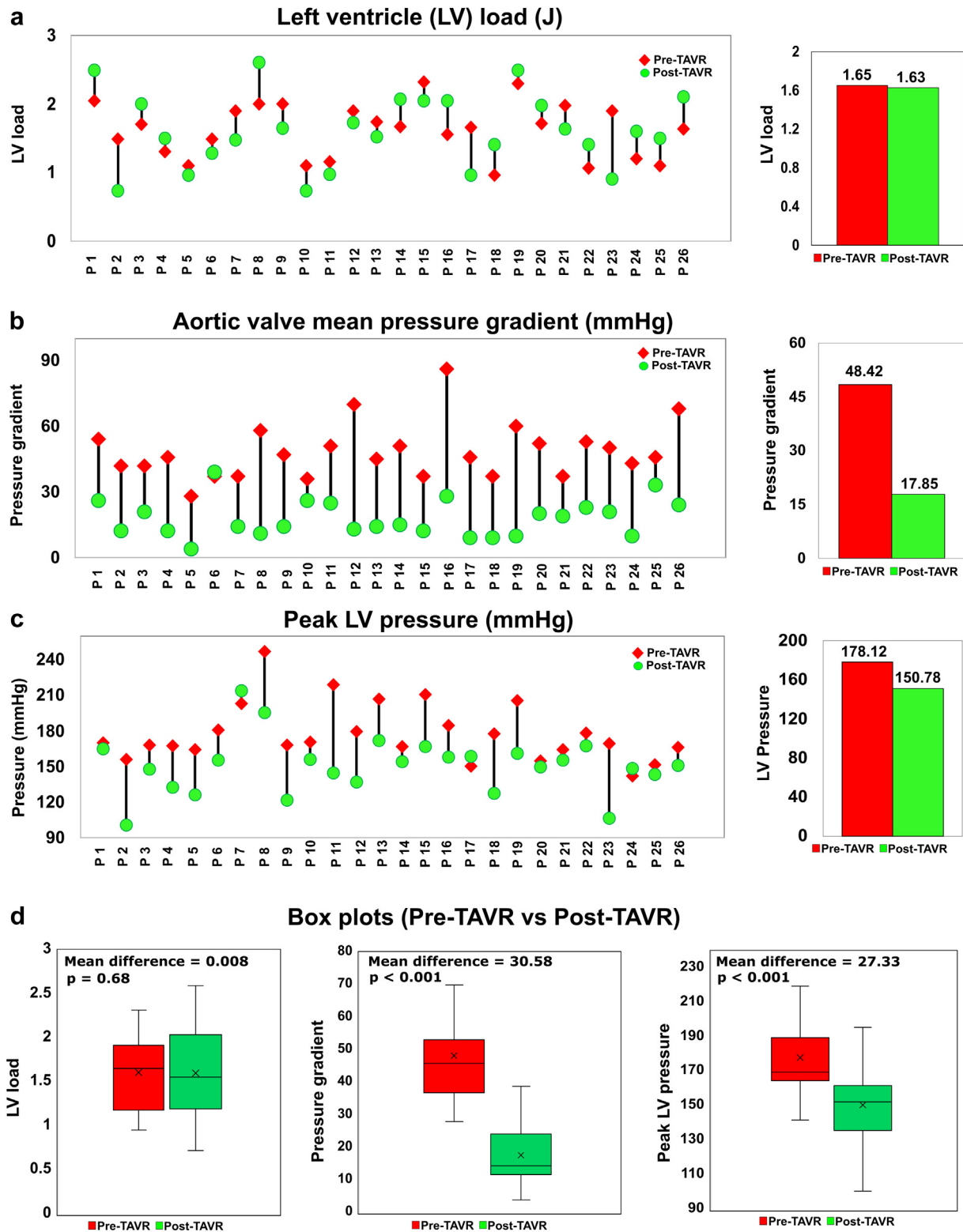


Figure 6. Global hemodynamics at baseline and post-TAVR (N = 26). (a) LV workload; (b) Aortic valve mean pressure gradient; (c) Ejection fraction; (d) Box plots comparing LV workload and clinical parameters pre- and post-TAVR. Abbreviations: LV, left ventricle; TAVR, transcatheter aortic valve replacement.

and global). As shown in [Figure 7a](#) and [b](#), NCC calcification volume was positively correlated with LCC blood stasis volume ($r = 0.43$; $p = 0.02$), whereas it was inversely correlated with commissural misalignment ($r = -0.534$; $p = 0.005$) after TAVR. Similarly, NCC calcium volume was

moderately correlated with RCC blood stasis volume pre-TAVR ($r = 0.457$; $p = 0.019$) as shown in [Figure 7c](#). Moreover, we observed ([Figure 7d](#)) a very strong negative correlation between total calcium volume and coronary resistance ($r = -0.652$; $p < 0.001$) as well as

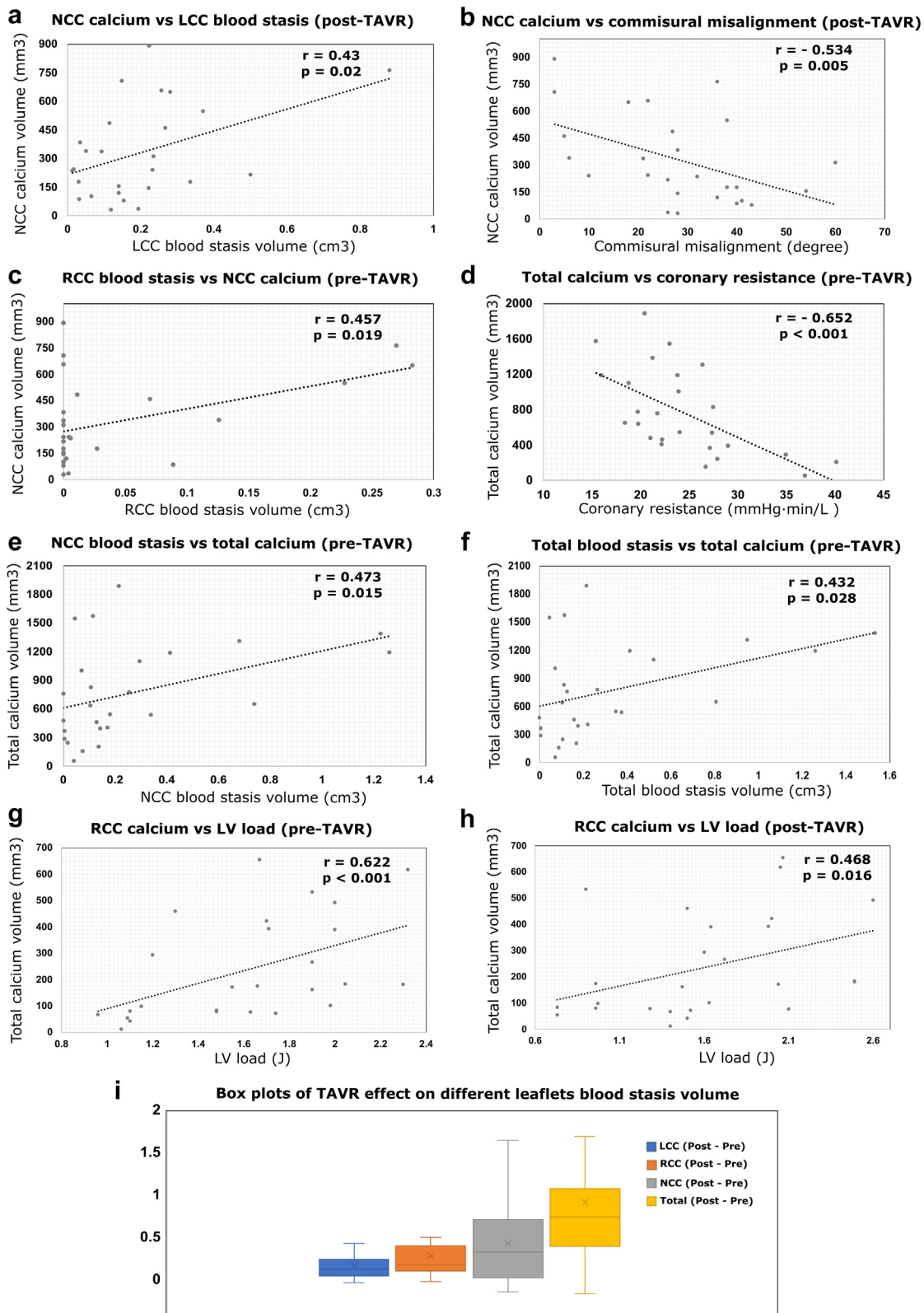


Figure 7. Correlation analysis between calcium volume of the leaflets and hemodynamic parameters (local and global) (N = 26). (a) Scatter plot of NCC calcium volume vs. LCC blood stasis volume (post-TAVR); (b) Scatter plot of NCC calcium volume vs. commissural misalignment (post-TAVR); (c) Scatter plot of NCC calcium volume vs. RCC blood stasis volume (pre-TAVR); (d) Scatter plot of total calcium volume vs. coronary resistance (pre-TAVR); (e) Scatter plot of total calcium volume vs. NCC blood stasis volume (pre-TAVR); (f) Scatter plot of total calcium volume vs. total blood stasis volume (pre-TAVR); (g) Scatter plot of RCC calcium volume vs. LV load (pre-TAVR); (h) Scatter plot of RCC calcium volume vs. LV load (post-TAVR); (i) Box plots comparing blood stasis volume changes after TAVR per leaflet for all patients.

Abbreviations: LCC, left coronary cusp; LV, left ventricle; NCC, noncoronary cusp; RCC, right coronary cusp; TAVR, transcatheter aortic valve replacement.

Table 1
Patient characteristics

Patient description	Pre-TAVR (n = 26, mean ± SD)	Post-TAVR (n = 26, mean ± SD)
Mean age (y)	76.3 ± 6.8	76.3 ± 6.8
Gender	(Male: 14; female: 12)	(Male: 14; female: 12)
Mean weight (kg)	87 ± 28.8	87 ± 28.8
Mean height (cm)	166.4 ± 10.11	166.4 ± 10.11
Society of Thoracic Surgeons score (%)	2.8 ± 1.84	2.8 ± 1.84
Body surface area (BSA)	1.90 ± 0.28	1.90 ± 0.28
Smoker	n = 6	n = 6
Prior atrial fibrillation (AF)	n = 4	N/A
Previous stroke	n = 3	N/A
Arterial hemodynamics		
Systolic arterial pressure (mmHg)	Pre-TAVR: 132 ± 19.72	Post-TAVR: 140 ± 24.45
Diastolic arterial pressure (mmHg)	Pre-TAVR: 69.7 ± 9.8	Post-TAVR: 72 ± 16.48
Coronary artery disease (CAD)	n = 5	n = 5
Hypertension (HTN)	n = 18	n = 18
Dyslipidemia	n = 10	n = 10
Prior coronary angiogram	n = 5	N/A
Coronary angiogram during TAVR	n = 12	n = 12
Prior percutaneous coronary intervention (PCI)	n = 4	N/A
Hemoglobin level (g/dL) (day of procedure)	132 ± 17	132 ± 17
Creatinine (mg/dL) (day of procedure)	82.71 ± 19.25	82.71 ± 19.25
Chronic kidney disease (CKD)	n = 4	n = 4
Chronic obstructive pulmonary disease (COPD)	n = 4	n = 4
Anticoagulation	n = 5	n = 5
Aortic valve hemodynamics		
Aortic valve area (cm ²)	Pre-TAVR: 0.82 ± 0.18	Post-TAVR: 1.68 ± 0.52
Aortic valve area index	Pre-TAVR: 0.43 ± 0.09	Post-TAVR: 0.89 ± 0.28
Stenotic aortic valve type	Tricuspid: 19; bicuspid: 7	Tricuspid: 26
Prosthetic size (mm)	N/A	25 ± 2.5
Prosthetic type		
Edwards SAPIEN 3	N/A	n = 26
Maximum aortic valve pressure gradient (mmHg)	Pre-TAVR: 84.66 ± 20.44	Post-TAVR: 27.8 ± 11.3
Mean aortic valve pressure gradient (mmHg)	Pre-TAVR: 48.42 ± 12.54;	Post-TAVR: 17.8 ± 8.34
Maximum aortic valve velocity (m/s)	Pre-TAVR: 4.57 ± 0.53;	Post-TAVR: 2.59 ± 0.51
Doppler velocity index (DVI)	Pre-TAVR: 0.25 ± 0.05	Post-TAVR: 0.48 ± 0.11
Pre-dilation	n = 5	N/A
Post-dilation	N/A	n = 4
Left ventricle and atrial hemodynamics		
Ejection fraction (%)	Pre-TAVR: 61 ± 7.9	Post-TAVR: 63.53 ± 7
Heart rate (bpm)	Pre-TAVR: 73 ± 13	Post-TAVR: 72 ± 12
LV mass index	Pre-TAVR: 93.36 ± 19.65	Post-TAVR: 93.27 ± 27.93
New onset atrial fibrillation (AF)	N/A	n = 4
New left bundle branch block (LBBB)	N/A	n = 6

LV, left ventricle; TAVR, transcatheter aortic valve replacement.

medium correlation between the total calcium score and both NCC and total blood stasis volumes pre-TAVR ($r = 0.473$; $p = 0.015$ NCC and $r = 0.432$; $p = 0.028$ total stasis volume) as shown in [Figure 7e](#) and [7f](#). Among other global hemodynamic metrics, we observed ([Figure 7g](#) and [h](#)) a strong correlation between the RCC calcium volume and the LV load in both pre- and post-TAVR states ($r = 0.622$; $p < 0.001$ pre-TAVR and $r = 0.468$; $p = 0.016$ post-TAVR). In summary, our findings showed that calcium volume score assessment could be an effective metric to predict future hemodynamic complication after TAVR. Additionally, we found that a substantial amount of calcium volume on the RCC leaflet is linked with a higher LV load.

Implantation Depth and Valve Size vs. Hemodynamic Parameters (Local and Global)

We examined the correlation between the valve size parameters including valve nominal area and area cover index as well as implantation depth with the hemodynamic parameters (please refer to [Supplemental Material](#) for the statistical analysis). We did not observe any significant correlation between valve size parameters and the stasis of blood flow (e.g., for total blood stasis and valve nominal area: $r = 0.18$; $p = 0.388$). We also did not observe any significant correlation between implantation depth and the stasis of blood flow. More specifically, the following statistical correlation results were observed between implantation depth and blood stasis regions per leaflet post-TAVR: $r = 0.224$ and

$p = 0.282$ for LCC blood stasis, $r = 0.053$ and $p = 0.802$ for RCC blood stasis, $r = 0.284$ and $p = 0.168$ for NCC blood stasis, and $r = 0.283$ and $p = 0.179$ for total blood stasis volume. In terms of coronary flow, based on the preliminary correlation analysis with all patient-specific variables against total mean coronary flow, we identified key parameters for multivariate regression as left coronary height, LV load, aortic root diameter, valve-to-left coronary distance and valve-to-right coronary distance. Overall, regression for total mean coronary flow pre-intervention was significant ($R^2 = 0.67$; $F(3, 22) = 14.6$; $p < 0.001$) with only the LV load being the significant predictor. Conversely, after intervention, the fitted model that included valve-to-coronary distances, implantation depth, and implanted valve size was found to be a better predictor for total mean coronary flow ($R^2 = 0.894$; $F(7, 17) = 20.4$; $p < 0.001$) with the strongest predictors being the valve-to-left coronary distance ($F = 8.813$; $p < 0.01$), LV load ($F = 7.824$; $p < 0.05$) and the aortic root diameter ($F = 4.5$; $p < 0.05$). The valve-to-right coronary distance, the left coronary height, implanted valve size, and depth did not significantly predict the total mean coronary flow.

In summary, our analysis revealed that the valve size and implanted depth are not independent significant predictors of local and global hemodynamic outcomes such as blood flow stasis, coronary flow, and LV load. However, we found that the valve-to-coronary distance, which is an indirect parameter linked to the proportion of valve size and aortic root size, could predict the coronary flow. In other words, not the valve size or implanted depth themselves, but the geometrical configuration

(and available space gap for fluid to flow) is a predictor of coronary flow after intervention. Therefore, a choice of larger valve size and over-expansion to prevent complications such as paravalvular leakage might end up with restricting the coronary blood flow.

Discussion

Within the native aortic valve and the aortic root, a whirling motion of the flow occurs along the sinuses of Valsalva which supplies the coronary arteries with blood during diastole and also helps to washout the blood from the sinus, preventing stagnation (Figure 2). Following intervention, TAVR implantation involves geometric components such as commissural misalignment, the depth of implantation, and misdirected deployment, which then affects the natural flow of blood in the sinus of Valsalva.⁴² This leads to a compromise between the flow of blood needing to reach the coronary circulation and the flow necessary for neo-sinus washout. The ramifications of this condition are still largely unstudied, and more research is necessary. It is important to quantify global and local flow,^{30,31} as this can help detect issues which standard anatomical assessments overlook.^{24,43} These alterations can result in thrombosis down the line (Figure 8), and would have likely gone undetected if a hemodynamic evaluation had not been done.⁴³

The purpose of this study was to determine whether the global and local hemodynamic disturbance caused by the geometrical configuration of transcatheter heart valves and their interactions with the coronary flow could potentially be the trigger point for subclinical valve thrombosis seen in some TAVR patients. We examined the correlation of detailed individualized geometrical factors after transcatheter heart valves deployment such as commissural misalignment, annular diameter, aortic root diameter, aorta angle, sinus diameter, valve size, implantation depth, valve to coronary distance, and coronary height as well as coronary hemodynamics on blood flow stasis in sinus and neo-sinus regions. In addition, we explored the leaflets calcification volumes correlation

with the global and local hemodynamic parameters. Our results showed that the risk of blood stasis in the aortic root and sinus is significantly higher after TAVR and is correlated with calcium volume distributions of leaflets before intervention. Additionally, we observed that TAVR can have adverse impact on the global and local hemodynamics for some patients, signifying the need for examining each patient individually. Our study presents several findings, each of which warrants individual discussion and consideration as outlined below.

TAVR Is Associated With High Risk of Blood Stagnation and Thrombosis in Sinus and Neo-Sinus Regions

When the transcatheter valve is deployed, the native leaflets and the prosthetic valve frame divide the area of natural sinus flow into 2 regions, a sinus and a neo-sinus, which results in a disturbance of the native flow.⁴⁴ The outcomes of our research demonstrate that TAVR alters the primary vortex pattern of the aortic root and sinus regions, leading to a reduction in the draining of sinus flow and the circulation of blood to the coronary arteries during diastole. We observed (Figure 2) that after TAVR, the native aortic root flow splits into 2 streams: one toward the coronaries (sinus) and the other one toward the aortic side of the bioprosthetic valve leaflets (neo-sinus). The swirling flow in the neo-sinus areas have a spin that is in the opposite direction to the original sinus flow, which has less power to transport the flow away from the leaflet roots, causing a substantially greater amount of stagnant blood after TAVR for all patients (Figures 2 and 4). While it has been reported that the possibility of blood flow stasis is roughly the same for LCC, RCC, and NCC neo-sinuses,⁴⁵ our research indicated that the likelihood of stasis varies with the amount of calcium and the deployment specifics. Specifically, the NCC neo-sinus is more prone to stagnant flow and is consequently more vulnerable to leaflet thrombosis than LCC and RCC. The inefficient sinus and neo-sinus washout along with increased blood stagnation increases the risk of thrombotic events after TAVR.^{46,47}

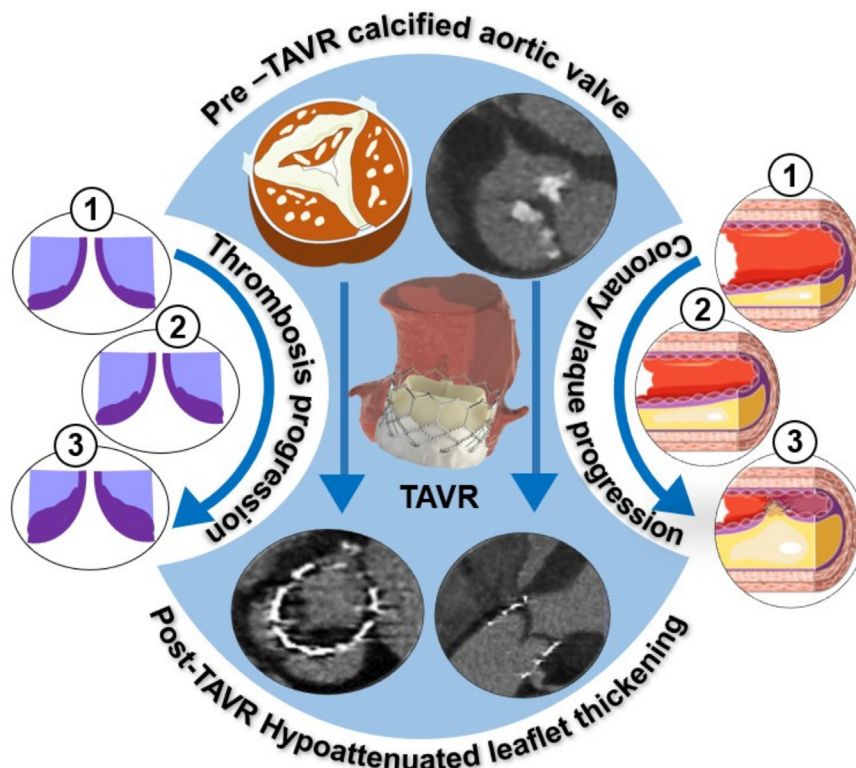


Figure 8. TAVR and the challenge of reducing the risk of leaflet thrombosis and coronary plaque progression over time.

Aortic Valve Calcium Volume Could Predict Significance of Post-TAVR Thrombosis and Cardiac Malfunction

With the increasing prevalence of TAVR, it is critical to evaluate the degree of calcification carefully as studies have shown that calcification of the aortic valve is connected to a variety of complications which may occur during and after the procedure.^{48,49} In particular, disproportional calcium volume of leaflets could restrict the optimal expansion of the prosthetic valve, leading to post-TAVR complications such as unequal neo-sinus volumes, asymmetrical leaflet expansion, and commissural misalignment.⁵⁰ Our results showed that asymmetrical calcium volume magnitude and its impact on implantation characteristics is directly linked to the blood stasis volume (local hemodynamic) and LV load (global hemodynamics) in both pre- and post-TAVR states (Figure 7). This could partially explain why TAVR might not be successful in terms of ventricle unloading in some patients with highly asymmetrical calcium volume or might be associated with thrombosis as a result of nonoptimal expansion.⁵¹

Coronary Flow Might Not Improve for Some Patients After TAVR

Excessive extravascular compressive forces resulting from AS reduce the amount of blood flow that reaches the LV through coronary perfusion pressure.⁵² After TAVR, a surge in pressure and flow downstream of the aortic valve is expected due to AS removal.⁵² Our results demonstrate that pressure and coronary flow do gain some improvement during systole. However, for many patients, diastolic flow of coronaries might not improve or may even drop. This reduction in coronary blood flow reduces the capacity to raise myocardial oxygenation, which can then lead to abnormal LV function, increased apoptosis (which can be connected to myocardial fibrosis and is an independent marker of mortality), and sudden death.^{52,53}

No Improvement in Left Ventricular Hemodynamics of Some Patients After TAVR

Measuring LV workload is an effective way to evaluate its performance, which is closely related to the severity of calcification in the aortic valve leaflets.²⁰ Increased workload can lead to cardiac remodeling that demands more oxygen from the myocardium, making it more susceptible to ischemia.⁵⁴ As the AS severity increases, the LV workload increases to make up for the decreased ejected flow, but after TAVR, a decrease in the workload is normally expected.²⁰ Despite this, our findings revealed that the decrease in the aortic valve pressure gradient post-TAVR was not necessarily associated with a decrease in workload for a majority of patients.

Another interesting finding of our study was that the RCC calcium volume was correlated with LV workload for both pre- and post-TAVR states. While we have previously shown the usefulness of LV load metric for TAVR patients,²⁰ this study demonstrated the significance of the interplay between LV load and asymmetric calcification severity. It is noteworthy that our results correspond to past studies which concluded that RCC calcium volume is an independent factor in determining LV dysfunction and the necessity of a pacemaker implant in patients who have undergone TAVR.⁵⁵

Conclusions




An optimal TAVR procedure strategy is subject-specific and is influenced by various factors that can impact sinus and neo-sinus hemodynamics, such as changes to the global circulatory system, the anatomy of the aortic root and aortic valve, coronary hemodynamics, and the presence of asymmetric valve calcification or incomplete prosthetic valve expansion. Nonuniform calcium distribution across the leaflets can prevent optimal TAVR expansion and lead to impaired flow washout toward

the coronary arteries, promoting subclinical leaflet thrombosis. This study suggests that particular attention should be paid to patients with significant asymmetry in calcification distribution or eccentric prosthetic valves postintervention, as they may be at increased risk of leaflet thrombosis and long-term coronary artery disease. In particular, valve thrombosis is associated with several potential risks, including thromboembolism, stroke, transient ischemic attack, and the risk of subsequent structural valve degeneration. The use of personalized computational simulations to simulate potential treatment options may assist interventional cardiologists in determining the best course of action and help to improve clinical outcomes for TAVR patients, as well as identify those at higher risk of future thrombosis or coronary artery disease.

Limitations

This study was performed and validated on 26 patients who underwent TAVR in both pre- and post-TAVR states (52 cases). Future studies must be conducted on a larger population of AS patients in both pre- and post-TAVR states to validate the clinical findings of this study. Another limitation of this study was that all patients were given the Edwards SAPIEN 3 balloon-expandable valve, meaning that the investigation of design factors was only done on that particular valve type. In the future, research will be conducted to include a wider range of self-expandable and balloon-expandable valves for the purpose of examining the effect of design factors on hemodynamic outcomes. Lastly, it is important to recognize the limitations of a retrospective study design and cautiously interpret the results. Nevertheless, since prospective studies require multiple post-TAVR CT scans, which can be quite risky, a retrospective study was seen as the best choice. Further research in this field, including properly planned prospective studies, would be beneficial for confirming and expanding upon the results of the present study.

ORCID

Seyedvahid Khodaei  <https://orcid.org/0000-0002-1311-9006>
 Mohamed Abdelkhalek  <https://orcid.org/0000-0002-8346-9087>
 Ali Emadi  <https://orcid.org/0000-0002-0676-1455>

Ethics Statement

Waiver of informed consent and data transfer was approved by the Institutional Review Boards of the institution (HiREB), Hamilton General Hospital. The selections were done by operators blinded to the objectives and contents of this study. Clinical measurements were performed per relevant guidelines and regulations including guidelines of the American College of Cardiology and American Heart Association.

Funding

This work was supported by NSERC Discovery Grant (RGPIN-2017-05349). NSERC (https://www.nserc-crsng.gc.ca/index_eng.asp) and the funders had no role in study design, data collection and analysis, decision to publish, or preparation of the manuscript.

Disclosure Statement

The authors report no conflict of interest.

Acknowledgments

The authors are highly thankful for the great comments of the 2 anonymous reviewers that helped us improve the quality of this article.

Supplementary Material

Supplemental data for this article can be accessed on the publisher's website.

References

- Abdul-Jawad Altisent O, Ferreira-Gonzalez I, Marsal JR, et al. Neurological damage after transcatheter aortic valve implantation compared with surgical aortic valve replacement in intermediate risk patients. *Clin Res Cardiol.* 2016;105:508-517.
- Athappan G, Gajulapalli RD, Sengodan P, et al. Influence of transcatheter aortic valve replacement strategy and valve design on stroke after transcatheter aortic valve replacement: a meta-analysis and systematic review of literature. *J Am Coll Cardiol.* 2014;63:2101-2110.
- Arora S, Ramm CJ, Misenerheimer JA, Vavalle JP. Early transcatheter valve prosthesis degeneration and future ramifications. *Cardiovasc Diagn Ther.* 2017;7:1-3.
- Bogyi M, Scherthner RE, Loewe C, et al. Subclinical leaflet thrombosis after transcatheter aortic valve replacement. *JACC Cardiovasc Interv.* 2021;14:2643-2656.
- Karady J, Apor A, Nagy AI, et al. Quantification of hypo-attenuated leaflet thickening after transcatheter aortic valve implantation: clinical relevance of hypo-attenuated leaflet thickening volume. *Eur Heart J Cardiovasc Imaging.* 2020;21:1395-1404.
- Garcia S, Fukui M, Dworak MW, et al. Clinical impact of hypoattenuating leaflet thickening after transcatheter aortic valve replacement. *Circ Cardiovasc Interv.* 2022;15:e011480.
- Makkar RR, Blanke P, Leipsic J, et al. Subclinical leaflet thrombosis in transcatheter and surgical bioprosthetic valves: PARTNER 3 cardiac computed tomography substudy. *J Am Coll Cardiol.* 2020;75:3003-3015.
- Blanke P, Leipsic JA, Popma JJ, et al. Bioprosthetic aortic valve leaflet thickening in the Evolut low risk sub-study. *J Am Coll Cardiol.* 2020;75:2430-2442.
- Yanagisawa R, Tanaka M, Yashima F, et al. Early and late leaflet thrombosis after transcatheter aortic valve replacement. *Circ Cardiovasc Interv.* 2019;12:e007349.
- Ruile P, Jander N, Blanke P, et al. Course of early subclinical leaflet thrombosis after transcatheter aortic valve implantation with or without oral anticoagulation. *Clin Res Cardiol.* 2017;106:85-95.
- Vollema EM, Kong WKF, Katsanos S, et al. Transcatheter aortic valve thrombosis: the relation between hypo-attenuated leaflet thickening, abnormal valve haemodynamics, and stroke. *Eur Heart J.* 2017;38:1207-1217.
- Oliveira DC, Okutucu S, Russo G, Martins ECC. The issue of subclinical leaflet thrombosis after transcatheter aortic valve implantation. *Cardiol Res.* 2020;11:269-273.
- Park D-W, Ahn J-M, Kang D-Y, et al. Edoxaban versus dual antiplatelet therapy for leaflet thrombosis and Cerebral thromboembolism after TAVR: the ADAPT-TAVR randomized clinical trial. *Circulation.* 2022;146:466-479.
- Nappi F, Mazzocchi L, Timofeva I, et al. A finite element analysis study from 3D CT to predict transcatheter heart valve thrombosis. *Diagnostics (Basel).* 2020;10:183.
- Ihdahyid AR, Sathananthan J. Patient-specific CT-Simulation in TAVR: an emerging guide in the lifetime journey of aortic valve disease. *J Cardiovasc Comput Tomogr.* 2022;16:e35-e37.
- Shen J, Faruqi AH, Jiang Y, Maftoon N. Mathematical reconstruction of patient-specific vascular networks based on clinical images and global optimization. *IEEE Access.* 2021;9:20648-20661.
- Kappetein AP, Head SJ, Généreux P, et al. Updated Standardized Endpoint Definitions for Transcatheter Aortic Valve Implantation: the valve Academic Research Consortium-2 Consensus Document††The valve Academic Research Consortium (VARC) Consists of Representatives From Several Independent Academic Research Organization, Several Surgery and Cardiology Societies, Members of the U.S. Food and Drug Administration (FDA), and Several Independents Experts. However, it is not a Society Document. Neither the Societies nor the FDA Have Been Asked to Endorse the Document. *J Am Coll Cardiol.* 2012;60:1438-1454.
- Nagueh SF, Bierig SM, Budoff MJ, et al. American society of echocardiography clinical recommendations for multimodality cardiovascular imaging of patients with hypertrophic cardiomyopathy: endorsed by the american society of nuclear cardiology, society for cardiovascular magnetic resonance, and society of cardiovascular computed tomography. *J Am Soc Echocardiogr.* 2011;24:473-498.
- Nagueh SF, Smiseth OA, Appleton CP, et al. Recommendations for the evaluation of left ventricular diastolic function by echocardiography: an update from the american society of echocardiography and the european association of cardiovascular imaging. *J Am Soc Echocardiogr.* 2016;29:277-314.
- Keshavarz-Motamed Z. A diagnostic, monitoring, and predictive tool for patients with complex valvular, vascular and ventricular diseases. *Sci Rep.* 2020;10:1-19.
- Baiocchi M, Barsoum S, Khodaei S, et al. Effects of choice of medical imaging modalities on a non-invasive diagnostic and monitoring computational framework for patients with complex valvular, vascular, and ventricular diseases who Undergo transcatheter aortic valve replacement. *Front Bioeng Biotechnol.* 2021;9:389.
- Khodaei S, Henstock A, Sadeghi R, et al. Personalized intervention cardiology with transcatheter aortic valve replacement made possible with a non-invasive monitoring and diagnostic framework. *Sci Rep.* 2021;11:10888.
- Ben-Assa E, Brown J, Keshavarz-Motamed Z, et al. Ventricular stroke work and vascular impedance refine the characterization of patients with aortic stenosis. *Sci Transl Med.* 2019;11:eav0181.
- Khodaei S, Garber L, Bauer J, Emadi A, Keshavarz-Motamed Z. Long-term prognostic impact of paravalvular leakage on coronary artery disease requires patient-specific quantification of hemodynamics. *Sci Rep.* 2022;12:21357.
- Bahadormanesh N, Tomka B, Kadem M, Khodaei S, Keshavarz-Motamed Z. An ultrasound-exclusive non-invasive computational diagnostic framework for personalized cardiology of aortic valve stenosis. *J Med Image Anal.* 2023;87:102795.
- Garber L, Khodaei S, Maftoon N, Keshavarz-Motamed Z. Impact of TAVR on coronary artery hemodynamics using clinical measurements and image-based patient-specific in silico modeling. *Nat Sci Rep.* 2023. <https://doi.org/10.1038/s41598-023-31987-w>
- Garber L, Khodaei S, Keshavarz-Motamed Z. The critical role of lumped parameter models in patient-specific cardiovascular simulations. *Arch Comput Methods Eng.* 2022;29:2977-3000.
- Asaadi M, Mawad W, Djebbari A, et al. On left ventricle stroke work efficiency in children with moderate aortic valve regurgitation or moderate aortic valve stenosis. *Pediatr Cardiol.* 2022;43:45-53.
- Keshavarz-Motamed Z, Garcia J, Gaillard E, et al. Effect of coarctation of the aorta and bicuspid aortic valve on flow dynamics and turbulence in the aorta using particle image velocimetry. *Exp Fluids.* 2014;55:1-16.
- Kadem M, Garber L, Abdelkhalek M, Al-Khazraji BK, Keshavarz-Motamed Z. Hemodynamic modeling, medical imaging, and machine learning and their applications to cardiovascular interventions. *IEEE Rev Biomed Eng.* 2023;16:403-423.
- Keshavarz-Motamed Z, del Alamo JC, Bluestein D, Edelman ER. Novel methods to advance diagnostic and treatment value of medical imaging for cardiovascular disease. *Front Bioeng Biotechnol.* 2022;10:1501.
- Keshavarz-Motamed Z, Nezami FR, Partida RA, et al. Elimination of transcoarctation pressure gradients has no impact on left ventricular function or aortic shear stress after intervention in patients with mild coarctation. *JACC Cardiovasc Interv.* 2016;9:1953-1965.
- Sadeghi R, Khodaei S, Ganame J, Keshavarz-Motamed Z. Towards non-invasive computational-mechanics and imaging-based diagnostic framework for personalized cardiology for coarctation. *Sci Rep.* 2020;10:9048.
- Keshavarz-Motamed Z, Garcia J, Gaillard E, et al. Non-invasive determination of left ventricular workload in patients with aortic stenosis using magnetic resonance imaging and Doppler echocardiography. *PLoS One.* 2014;9:e86793.
- Sadeghi R, Gasner N, Khodaei S, Garcia J, Keshavarz-Motamed Z. Impact of mixed valvular disease on coarctation hemodynamics using patient-specific lumped parameter and Lattice Boltzmann modeling. *Int J Mech Sci.* 2022;217:107038.
- Sadeghi R, Tomka B, Khodaei S, Garcia J, Ganame J, Keshavarz-Motamed Z. Reducing morbidity and mortality in patients with coarctation requires systematic differentiation of impacts of mixed valvular disease on coarctation hemodynamics. *J Am Heart Assoc.* 2022;11:e022664.
- Sadeghi R, Tomka B, Khodaei S, et al. Impact of extra-anatomical bypass on coarctation fluid dynamics using patient-specific lumped parameter and Lattice Boltzmann modeling. *Sci Rep.* 2022;12:9718.
- Khodaei S, Sadeghi R, Blanke P, Leipsic J, Emadi A, Keshavarz-Motamed Z. Towards a non-invasive computational diagnostic framework for personalized cardiology of transcatheter aortic valve replacement in interactions with complex valvular, ventricular and vascular disease. *Int J Mech Sci.* 2021;202-203:106506.
- Keshavarz-Motamed Z, Khodaei S, Rikhtegar Nezami F, et al. Mixed valvular disease following transcatheter aortic valve replacement: quantification and systematic differentiation using clinical measurements and image-based patient-specific in silico modeling. *J Am Heart Assoc.* 2020;9:e015063.
- Singh-Gryzbos S, Ncho B, Sadri V, et al. Influence of patient-specific characteristics on transcatheter heart valve neo-sinus flow: an in silico study. *Ann Biomed Eng.* 2020;48:2400-2411.
- Raghav V, Clifford C, Midha P, Okafor I, Thurow B, Yoganathan A. Three-dimensional extent of flow stagnation in transcatheter heart valves. *J R Soc Interface.* 2019;16:20190063.
- Kaneko T. Flow in the aortic sinus after valve-in-valve TAVR. *JACC Cardiovasc Interv.* 2021;14:2667-2669.
- Farag ES, Vendrik J, van Ooij P, et al. Transcatheter aortic valve replacement alters ascending aortic blood flow and wall shear stress patterns: a 4D flow MRI comparison with age-matched, elderly controls. *Eur Radiol.* 2019;29:1444-1451.
- Midha PA, Raghav V, Sharma R, et al. The fluid mechanics of transcatheter heart valve leaflet thrombosis in the Neosinus. *Circulation.* 2017;136:1598-1609.
- Trusty PM, Bhat SS, Sadri V, et al. The role of flow stasis in transcatheter aortic valve leaflet thrombosis. *J Thorac Cardiovasc Surg.* 2022;164:e105-e117.
- Toninato R, Salmon J, Susin FM, Ducci A, Burriesci G. Physiological vortices in the sinuses of Valsalva: an in vitro approach for bio-prosthetic valves. *J Biomech.* 2016;49:2635-2643.
- Pott D, Sedaghat A, Schmitz C, et al. Hemodynamics inside the neo- and native sinus after TAVR: effects of implant depth and cardiac output on flow field and coronary flow. *Artif Organs.* 2021;45:68-78.
- Pollari F, Hitzl W, Vogt F, et al. Aortic valve calcification as a risk factor for major complications and reduced survival after transcatheter replacement. *J Cardiovasc Comput Tomogr.* 2020;14:307-313.
- Abdelkhalek M, Daeian MA, Chavarria J, et al. Patterns and Structure of Calcification in Aortic Stenosis: An Approach on Contrast-Enhanced CT Images. *JACC Cardiovasc Imag.* Published online April 12, 2023; <https://doi.org/10.1016/j.jcmg.2023.02.011>
- Fukui M, Bapat VN, Garcia S, et al. Deformation of transcatheter aortic valve prostheses: Implications for hypoattenuating leaflet thickening and clinical outcomes. *Circulation.* 2022;146:480-493.
- Milhorini Pio S, Bax J, Delgado V. How valvular calcification can affect the outcomes of transcatheter aortic valve implantation. *Expert Rev Med Devices.* 2020;17:773-784.
- McConkey HZR, Marber M, Chiribiri A, Pibarot P, Redwood SR, Prendergast BD. Coronary microcirculation in aortic stenosis. *Circ Cardiovasc Interv.* 2019;12:e007547.
- Heusch G. Myocardial ischemia: lack of coronary blood flow, myocardial oxygen supply-demand imbalance, or what? *Am J Physiol Heart Circ Physiol.* 2019;316:H1439-H1446.
- Banerjee P. Heart failure: a story of damage, fatigue and injury? *Open Heart.* 2017;4:e000684.
- Spaziano M, Chieffo A, Watanabe Y, et al. Computed tomography predictors of mortality, stroke and conduction disturbances in women undergoing TAVR: a sub-analysis of the WIN-TAVI registry. *J Cardiovasc Comput Tomogr.* 2018;12:338-343.